laparoscopic approach, a repeatedly reported advantage of laparoscopic surgery [5, 12–14]. Laparoscopic surgery is expected to have many other advantages owing to its minimal invasiveness, including reduced incidence of infertility [16, 17] and desmoid tumors [27, 28]. Although these advantages are yet to be proven, they may contribute when patients and surgeons decide to perform surgical interventions when patients are younger.

We clarified the time trend of surgical treatment for FAP and its clinical relevance in Japan based on one of the largest and recent series of FAP patients. The introduction of laparoscopic surgery altered clinical practice regarding surgical treatments for FAP patients. We observed no adverse clinical outcomes associated with the increased use of laparoscopic surgery, excluding two-stage surgery, indicating that prophylactic surgical intervention may be performed either laparoscopically or with open surgery with equivalent outcome through experienced hands. Nevertheless, we would like to emphasize that the efficacy and safety of laparoscopic surgery for FAP has not been established yet. Future appropriately planned clinical trials exclusively comprising patients with FAP and focusing on the clinical utility of the laparoscopic approach regarding specific postoperative complications, long-term outcomes of quality of life, and costs are required. Such studies may validate the clinically important concept of minimally invasive techniques and thereby lowering the risk of postoperative intra-abdominal desmoid tumors [20, 24].

Compliance with ethical standards

Conflict of interest The authors declare that they have no conflict of interest.

References

1. Vasen HFA, Möslein G, Alonso A et al (2008) Guidelines for the clinical management of familial adenomatous polyposis (FAP). Gut 57:704–713
2. Wexner SD, Jahansen OB, Nogueras JJ et al (1992) Laparoscopic total abdominal colectomy. a prospective trial. Dis Colon Rectum 35:651–655
3. Maartense S, Dunker MS, Slors JF et al (2004) Hand-assisted laparoscopic versus open restorative proctocolectomy with ileal pouch anal anastomosis. Ann Surg 2004:984–992
4. Kienle P, Z'graggen K, Schmidt J et al (2005) Laparoscopic restorative proctocolectomy. Br J Surg 92:88–93
5. Schiessling S, Leowardi C, Kienle P et al (2013) Laparoscopic versus conventional ileoanal pouch procedure in patients undergoing elective restorative proctocolectomy (LapConPouch Trial)—a randomized controlled trial. Langenbecks Arch Surg 398:807–816
6. Larson DW, Cima RR, Dozois EJ et al (2006) Safety, feasibility, and short-term outcomes of laparoscopic ileal-pouch-anal anastomosis. a single institutional case-matched experience. Ann Surg 243:667–672
7. Lefevre JH, Bretagnol F, Ouaïssi M et al (2009) Total laparoscopic ileal pouch-anal anastomosis: prospective series of 82 patients. Surg Endosc 23:166–173
8. McNicol FJ, Kennedy RH, Philips RKS et al (2011) Laparoscopic total colectomy and ileorectal anastomosis (IRA), supported by an increased recovery programme in cases of familial adenomatous polyposis. Colorectal Dis 14:458–462
9. Vitellaro M, Bonfanti G, Sala P et al (2011) Laparoscopic colectomy and restrative proctocolectomy for familial adenomatous polyposis. Surg Endosc 25:1866–1875
10. Campos FG, Araújo SE, Melani AG et al (2011) Surgical outcomes of laparoscopic colorectal resections for familial adenomatous polyposis. Surg Laparosc Endosc Percutan Tech 21:327–333
11. Kim HJ, Choi G-S, Park JS et al (2012) Early postoperative and long-term oncological outcomes of laparoscopic treatment for patients with familial adenomatous polyposis. J Korean Surg Soc 83:288–297
12. Dunker MS, Bemelman WA, Slors JFM et al (2001) Functional outcome, quality of life, body image, and cosmesis in patients after laparoscopic-assisted and conventional restorative proctocolectomy. a comparative study. Dis Colon Rectum 44:1800–1807
13. Polle SW, Dunker MS, Slors JFM et al (2007) Body image, cosmesis, quality of life, and functional outcome of hand-assisted laparoscopic versus open restorative proctocolectomy: long-term results of a randomized trial. Surg Endosc 21:1301–1307
14. AhmedAli U, Keus F, Heikens JT et al (2009) Open versus laparoscopic (assisted) ileo pouch anal anastomosis for ulcerative colitis and familial adenomatous polyposis. Cochrane Database Syst Rev 1:CD006267
15. Marcello PW, Milsom JW, Wong SK et al (2000) Laparoscopic restorative proctocolectomy. Case-matched comparative study with open restorative proctocolectomy. Dis Colon Rectum 43:604–608
16. Bartels SAL, D'Hoore A, Cuesta MA et al (2012) Significantly increased pregnancy rates after laparoscopic restorative proctocolectomy: a cross-sectional study. Ann Surg 256:1045–1048
17. Beyer-Berjot L, Maggiori L, Birnbaum D et al (2013) A total laparoscopic approach reduces the infertility rate after ileal pouch-anal anastomosis. A 2-center study. Ann Surg 258:275–282
18. Ganschow P, Warth R, Hinz U et al (2013) Early postoperative complications after stapled vs handsewn restorative proctocolectomy with ileal pouch-anal anastomosis in 148 patients with familial adenomatous polyposis coli: a matched-pair analysis. Colorectal Dis 16:116–122
19. Japanese Society for Cancer of the Colon and Rectum (2012) JSCCR guidelines 2012 for the clinical practice of hereditary colorectal cancer. Kanehara and Co., Ltd, Tokyo
20. Church J, Simmang C (2003) Practice parameters for the treatment of patients with dominantly inherited colorectal cancer (familial adenomatous polyposis and hereditary nonpolyposis colorectal cancer). Dis Colon Rectum 46:1001–1012
21. Moreira AL, Church JM, Burke CA (2009) The evolution of prophylactic colorectal surgery for familial adenomatous polyposis. Dis Colon Rectum 52:1481–1486
22. Aziz O, Athanasiou T, Fazio VW et al (2006) Meta-analysis of observational studies of ileorectal versus ileal pouch-anal anastomosis for familial adenomatous polyposis. Br J Surg 93:407–417
23. Iwama T, Tamura K, Morita T et al (2004) A clinical overview of familial adenomatous polyposis derived from the database of the polyposis registry of Japan. Int J Clin Oncol 9:308–316
24. Kartheuser A, Stangherlin P, Brandt D et al (2006) Restorative proctocolectomy and ileal pouch-anal anastomosis for familial adenomatous polyposis revisited. Fam Cancer 5:241–260

25. Hor T, Zalinski S, Lefevre JH et al (2012) Feasibility of laparoscopic restorative proctocolectomy without diverting stoma. Dig Liver Dis 44:118–122
26. Kennedy RD, Zarroug AE, Moir CR et al (2014) Ileal pouch anal anastomosis in pediatric familial adenomatous polyposis: a 24-year review of operative technique and patient outcomes. J Pediat Surg 49:1409–1412
27. Vitellaro M, Ferrari A, Trencheva K et al (2012) Is laparoscopic surgery an option to support prophylactic colectomy in adolescent patients with familial adenomatous polyposis (FAP)? Pediatr Blood Cancer 59:1223–1228
28. Vitellaro M, Sala P, Signoroni S et al (2014) Risk of desmoid tumours after open and laparoscopic colectomy in patients with familial adenomatous polyposis. Br J Surg 101:558–565

Familial Cancer
DOI 10.1007/s10689-016-9872-x

ORIGINAL ARTICLE

Rapid detection of germline mutations for hereditary gastrointestinal polyposis/cancers using HaloPlex target enrichment and high-throughput sequencing technologies

Masakazu Kohda[1] · Kensuke Kumamoto[2,3] · Hidetaka Eguchi[1] · Tomoko Hirata[1] · Yuhki Tada[1] · Kohji Tanakaya[4] · Kiwamu Akagi[5] · Seiichi Takenoshita[3] · Takeo Iwama[2] · Hideyuki Ishida[2] · Yasushi Okazaki[1]

Abstract Genetic testing for hereditary colorectal polyposis/cancers has become increasingly important. Therefore, the development of a timesaving diagnostic platform is indispensable for clinical practice. We designed and validated target enrichment sequencing for 20 genes implicated in familial gastrointestinal polyposis/cancers in 32 cases with previously confirmed mutations using the HaloPlex enrichment system and MiSeq. We demonstrated that HaloPlex captured the targeted regions with a high efficiency (99.66 % for covered target regions, and 99.998 % for breadth of coverage), and MiSeq achieved a high sequencing accuracy (98.6 % for the concordant rate with SNP arrays). Using this approach, we correctly identified 33/33 (100 %) confirmed alterations including SNV, small INDELs and large deletions, and insertions in *APC, BMPR1A, EPCAM, MLH1, MSH2, MSH6, PMS2,* and *SKT11*. Our approach yielded the sequences of 20 target genes in a single experiment, and correctly identified all previously known mutations. Our results indicate that our approach successfully detected a wide range of genetic variations in a short turnaround time and with a small sample size for the rapid screening of known causative gene mutations of inherited colon cancer, such as familial adenomatous polyposis, Lynch syndrome, Peutz–Jeghers syndrome, and Juvenile polyposis syndrome.

Keywords Hereditary gastrointestinal polyposis · Colorectal cancer · Familial adenomatous polyposis · Lynch syndrome · Mismatch repair genes

Masakazu Kohda and Kensuke Kumamoto are identical first authors.

Electronic supplementary material The online version of this article (doi:10.1007/s10689-016-9872-x) contains supplementary material, which is available to authorized users.

✉ Hideyuki Ishida
05hishi@saitama-med.ac.jp

✉ Yasushi Okazaki
okazaki@saitama-med.ac.jp

1 Division of Translational Research, Research Center for Genomic Medicine, Saitama Medical University, 1397-1 Yamane, Hidaka, Saitama 350-1241, Japan

2 Department of Digestive Tract and General Surgery, Saitama Medical Center, Saitama Medical University, Kamoda, Kawagoe City, Saitama 350-8550, Japan

3 Department of Organ Regulatory Surgery, Fukushima Medical University, Fukushima 960-1295, Japan

4 Department of Surgery, Iwakuni Clinical Center, Yamaguchi 740-8510, Japan

5 Divisions of Molecular Diagnosis and Cancer Prevention, Saitama Cancer Center, Saitama 362-0806, Japan

Introduction

Hereditary gastrointestinal cancer syndromes (HGICS) represent a phenotypically diverse group of disorders that exhibit distinct patterns of inheritance in an individual's progeny [1]. They are composed of various syndromes such as Lynch syndrome (LS), familial adenomatous syndrome (FAP), MUTYH-associated polyposis (MAP), Peutz–Jeghers syndrome (PJS), juvenile polyposis syndrome (JPS), Cowden syndrome (CS), serrated (hyperplastic) polyposis syndrome (SPS), Li–Fraumeni syndrome (LFS), hereditary diffuse gastric cancer (HDGC), and gastric adenocarcinoma and proximal polyposis of the stomach (GAPPS) [1, 2]. In addition, a recent advance in molecular biology has enabled the identification of another member of HGICS, polymerase proofreading-associated syndrome (PPAS), that harbors germline mutations affecting the proofreading domains of

Published online: 02 February 2016

POLE and POLD1 by means of whole genome sequencing [3]. Since different HGICSs (i.e., mild FAP, MAP, and PPAS) share their clinical phenotypes, molecular genetic studies becomes increasingly important for differential diagnosis and for assessing the risk of recurrence [4].

Traditional molecular diagnosis based on the Sanger-sequencing technique, which is typically performed by sequencing several candidate genes in order, is quite time-consuming and labor-intensive, making it difficult to apply routinely for the diagnosis of some HGICSs. To overcome these obstacles, diagnostics using high-throughput sequencing techniques have been introduced [5] and have become an important part of clinical genetic testing [6].

One of the key features of high-throughput sequencing-based diagnostics is its ability to detect a wide range of genetic variation, such as a single nucleotide variant, small insertions and deletions, large exonic deletions and duplications, and translocation. Most reports thus far have utilized HiSeq, a powerful and efficient ultra-high-throughput sequencing system, for this purpose [5, 7, 8]. On the other hand, a bench-top high-throughput sequencer, such as MiSeq, has the advantages of fast sequencing turnover times (less than 40 h per running) and cost-reduction for a single run, and thus is ideal for use in small clinical laboratories [9]. For library preparation, several methods are available that are based on hybrid capture or circularization with PCR for the target enrichment of genomic DNA regions [10]. Among these methods, we chose the HaloPlex technique, which uses a selective circularization method; the genomic DNA was digested with 16 different restriction enzymes, followed by the capture of DNA fragments from the targeted gene regions. HaloPlex was developed to simplify laboratory procedures, compared with other capture-based enrichment technologies, and requires only small amounts of starting DNA. We combined this enrichment system and bench-top MiSeq sequencer to realize genetic testing with a small sample size and a short turnaround time. In the present study, we show the results of our approach using a series of 32 Japanese patients with familial colorectal cancers and polyposis.

Materials and methods

Study subjects

The participants were 32 patients diagnosed as having hereditary colorectal polyposis/cancers syndromes with a known mutation in one of eight genes (*APC, BMPR1A, EPCAM, MLH1, MSH2, MSH6, PMS2,* or *SKT11*). The clinical diagnoses of these patients were FAP in 18 patients, LS in 12 patients, JPS in one patient, and PJS in one patient. Clinical diagnosis of each patient was compatible with the result of genetic mutations. Variations that likely affect functions for each patient had been previously identified using the Sanger sequencing of PCR amplicons or by multiplex ligation-dependent probe amplification. Five Japanese HapMap DNA samples (NA18942, NA18945, NA18953, NA18959, and NA18974) were obtained from Coriell Cell Repositories (Camden, New Jersey).

Ethical considerations

Informed consent was obtained from each participant. This research was approved by the Institutional Review Board at Saitama Medical Center, Saitama Medical University (926), and the Ethics Committee at Saitama Medical University (592-II) and was conducted according to the guidelines put forth in the Declaration of Helsinki.

DNA extraction, quantification, and quality control

DNA was extracted from whole blood using a QIAamp DNeasy blood and tissue DNA extraction kits (Qiagen, Valencia, CA), according to the manufacturer's documentation.

The purity and concentration of the extracted DNA were measured using a NanoDrop 1000 spectrophotometer (Thermo Scientific, Wilmington, DE) and a Qubit fluorometer (Life Technologies, Carlsbad, CA) for all the samples. All the samples fulfilled the minimum quality and purity requirements of 1 mg in less than a 130-mL volume, with an optical density OD260/280 of 1.7–1.9 and an OD260/230 of >2. A260/A280 ratios of 1.8–2.0 and A260/A230 ratios >1.5 were accepted. DNA fragmentation was assessed using agarose gel (2 %) electrophoresis.

Targeted capture and sequencing

A library of all the coding exons and intron–exon boundaries of 19 known genes (*BMPR1A, CDH1, EPCAM, MBD4, MLH1, MLH3, MSH2, MSH3, MSH6, MUTYH, PMS1, PMS2, POLD1, POLE, PTEN, SMAD4, STK11, TGFBR2,* and *TP53*) and the'entire genomic sequence of *APC* was prepared using HaloPlex target enrichment kits (Agilent Technologies, Santa Clara, USA), according to the manufacturer's instructions. Approximately 225 ng of DNA was fragmented using restriction enzymes. The probes with sequence indexes were added and hybridized to the targeted fragments. Each probe was an oligonucleotide designed to hybridize to both ends of a targeted DNA restriction fragment, thereby guiding the targeted fragments to form circular DNA molecules. The HaloPlex probes were biotinylated, and the targeted fragments were then retrieved with magnetic streptavidin beads. Small fragments of 150 bp and unligated probes were removed

from the mix by AMPure purification (Agencourt Bioscience, Beverly, MA, USA). Next, the circular molecules were closed by ligation. Finally, the enriched DNA fragments were amplified using universal primers. The enriched library concentration was estimated using a library quantification kit (Kapa Biosystems, Wilmington, MA). High-throughput sequencing was performed with 150-bp paired-end reads on a MiSeq platform (Illumina, Inc., San Diego, CA) for each enriched library according to the manufacturers' protocols.

Sequence data analysis

The raw sequence read data passed the quality checks in FASTQC (http://www.bioinformatics.babraham.ac.uk/projects/fastqc). Read trimming via base quality was performed using Trimmomatic [11].

Read alignments to the 1000 Genomes Project phase II reference genome (hs37d5.fa) were performed using the Burrows-Wheeler Aligner [12] (BWA, version 0.7.10-r789). Non-mappable reads were removed using SAMtools [13] (version 0.1.19-44428cd). After filtering out those reads, we applied the Genome Analysis Toolkit [14] (GATK version 3.3-0-g37228af) local realignment, base quality score recalibration, and single nucleotide variants (SNV) and small insertions and deletions (INDEL) discovery (HaplotypeCaller). Detected variants were annotated using ANNOVAR [15] (version 2015 March). The hybrid selection performances were evaluated using the Picard program (http://broadinstitute.github.io/picard/).

Variant prioritization

Variants were prioritized according to the following strategies (Supplementary Fig. S1). We only retained variants predicted to affect protein function; these included nonsense, splice site, coding indel, or missense variants. To remove polymorphisms, these variants were compared with the NHLBI Exome Sequencing Project (ESP; Seattle, WA, last accessed April 2015; http://evs.gs.washington.edu/EVS/) and Human Genetic Variation Database (HGVD; genetic variations determined by exome sequencing of 1208 individuals in Japan; http://www.genome.med.kyoto-u.ac.jp/SnpDB/index.html). We removed variants with a minor allele frequency (MAF) of >5 % for ESP6500, and >5 % in HGVD. Variants identified in HapMap [16] samples and that were too common among the cases were also excluded. The mutation databases, InSight (International Society for Gastrointestinal Hereditary Tumors; http://www.insight-group.org/ mutations) [17] and HGMD (Human Gene Mutation Database professional version; last accessed January 2015; http://www.biobase-international.com/product/hgmd) [18] were also used in a search for known pathogenic mutations. All the analyses were performed in a blinded manner.

Deletion and duplication call

Duplications and deletions of exons were detected by a depth of coverage analysis using custom ruby scripts and R (http://www.R-project.org/). The depth of coverage was obtained from mapped sequence data using BEDtools (version 2.23.0) [19]. The read depth of each base was divided by the total depth for normalization and each individual's normalized read depth was then compared to the average of the normalized read depth. The derived ratio was compared with threshold ratios <0.6 for deletions and >1.4 for duplications. Identified duplications and deletions were plotted using a ggbio package [20]. The regions where copy number changes were common among the cases were excluded for further investigation, because they are likely to cause artefacts.

Structure variation call

Clipping reveals structure (CREST) program [21] was applied to identify structure variations (large insertion, inversion, and translocation) using soft-clipping reads information. CREST assembles soft-clipped reads, and remaps the assembled sequence to identify breakpoints of structural variations at the nucleotide level of resolution. CREST.pl was executed with the following options: norm_tandem_repeat, normdup, and min_sclip_reads 10. After all the samples were processed, we removed variations with a low coverage and common variations among the samples. Consensus sequences were obtained from the output file of the CREST.pl. BLAT, UCSC Genome Browser [22], and the Integrated Genome Viewer [23] was used for manual curation.

Results

Design of this study

To develop a more convenient system for the clinical diagnosis of hereditary colon cancer than those reported so far, we applied the HaloPlex technique and the MiSeq sequencing system. MiSeq is a small-size high-throughput sequencer that produces an approximately 4.5-Gb sequence per run (MiSeq Reagent Kit v2). We applied the HaloPlex technique for targeted enrichment, since it requires only a small amount of DNA (225 ng) to start and the library preparation system is suitable for manual operation when the sample size is not sufficiently large. We designed target

regions to enrich all the coding exons and exon–intron junctions of 19 disease-causing genes and the entire *APC* gene to achieve effective screening (Table 1). The mean percentile of covered target regions was 99.66 %.

The workflow of our approach (HaCo-Seq) is summarized in Fig. 1. The detailed mutation screening process was also outlined in Fig. S1. Variants were identified and prioritized as described in the Materials and Methods section.

Quality assessment

A median of 2479,000 sequence reads was obtained per sample (ranging from 1,867,000 to 3,563,000 reads/sample), and the on-target rate (percentage of reads that were mapped to target regions) was 84.0 %. Of the designed targeted bases, 99.998 % had a minimum of 30-fold coverage, and a mean depth of 1203-fold (ranging from 0 to 3740-fold) coverage per nucleotide across the coding regions of the target genes was obtained per run (Fig. S2), as calculated using a representative run containing 11 multiplexed samples.

Identification of SNVs and INDELs

We mapped the sequences produced from 32 cases and 5 controls to the reference human genome and extracted 672

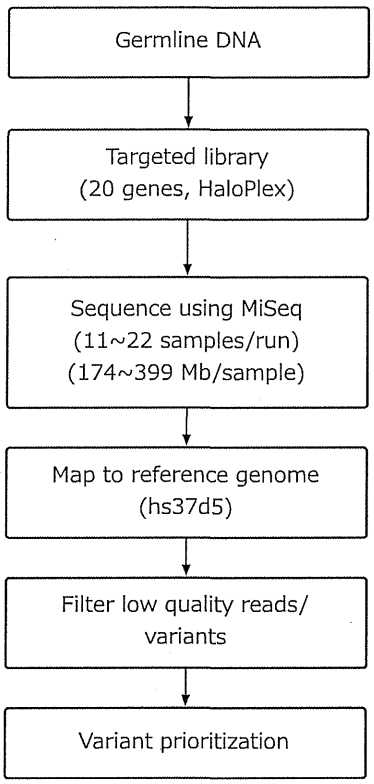

Fig. 1 Workflow of screening for mutations in colon cancer genes using high-throughput sequencing

Table 1 Genomic regions targeted in this study

Symbol	Location (hg19)	Target region (bp)	Covered region (%)
APC	chr5:112043184-112203289	1,60,105	98.8
BMPR1A	chr10:88635765-88683486	1819	100
CDH1	chr16:68771308-68868194	3135	99.7
EPCAM	chr2:47596204-47613762	1533	100
MBD4	chr3:129150333-129158686	1957	100
MLH1	chr3:37035028-37107120	2711	100
MLH3	chr14:75483774-75516368	4709	99.9
MSH2	chr2:47630320-47739583	3344	99.7
MSH3	chr5:79950536-80171691	3894	100
MSH6	chr2:48010362-48034009	4318	100
MUTYH	chr1:45794967-45805936	2140	100
PMS1	chr2:190656525-190742172	3397	99.3
PMS2	chr7:6013019-6048660	2889	98
POLD1	chr19:50902095-50921214	3847	100
POLE	chr12:133201272-133413397	8171	99.9
PTEN	chr10:89624216-89725239	1392	100
SMAD4	chr18:48573406-48604847	1999	100
STK11	chr19:1206902-1226656	1482	100
TGFBR2	chr3:30648365-30733101	2067	100
TP53	chr17:7565246-7579922	1697	97.9

variants (538 SNVs and 134 INDELs) predicted to affect protein functions for further analysis. After filtering processes, 56 prioritized variants (31 SNVs and 25 INDELs) remained in total. All 56 variants are listed in Supplementary Table S1. The number of remaining variants ranged from 1 to 3 per patient across 20 genes. Twenty-five confirmed alterations that could affect functions, were correctly detected in *APC, BMPR1A, MLH1, MSH2, MSH6,* and *PMS2* genes from patients (Table 2). The identified INDEL sizes ranged from 1 to 9 bp. All confirmed mutations were tested in a blinded fashion. Collectively, we correctly identified 25 previously confirmed 7 SNVs and 18 INDELs (25/25, 100 %).

Identification of exonic deletions and duplications

In addition to SNVs and INDELs, we also correctly identified confirmed exonic deletions and a duplication by comparing the sequence depth of each sample within the same sequence run. The copy number change criteria were such that the sequence depth was <60 % or >140 % of the normalized coverage of depth as calculated using the average depth of all the samples in the experiment. Commonly identified duplication/deletions among samples were excluded from further considerations. This simple approach accurately detected six confirmed exonic deletions and one genomic duplication (Fig. 2).

Structure variations

To identify other structure variations (large insertion, inversion, translocation), we performed a soft-clipped reads analysis using the CREST program [21]. One candidate for a structure variation was detected in subject GSS-49. An assembled sequence of the soft-clipped sequences was at least 38 bp in length, and was inserted in the last exon of *MSH6* (5′-CTAGTGAAAGGTCAACTGTAGATGCTGAAGCTGTCCAT-3′) (Fig. 3a). This inserted sequence turned out to be derived from upstream of the left breakpoint, as determined by a sequence analysis using UCSC BLAT (Kent, 2002), and was located in tandem with the original genomic sequence (Fig. 3b). Because of the 150-bp sequence read length, we could only determine the left breakpoint in an analysis of the current sequence data.

Reproducibility between runs

To test the between-run reproducibility, we sequenced 6 samples twice in independent runs. The numbers of reads were down sampled to remove biases on variant calling across the same DNA.

The test was performed based on the following criteria: (1) use of variants (SNV and INDEL) located in exons or exon–intron junctions, (2) removal of variants with a low depth of coverage (<20) and/or other low-quality factors related to variant calling, and (3) independent library construction and sequencing. Under these conditions, the variation consistencies for each of the samples were 98.7 % (77/78) for GSS-02, 98.7 % (77/78) for GSS-03, 98.7 % (77/78) for GSS-08, 98.7 % (78/79) for GSS-43, 100 % (79/79) for GSS-44, and 98.7 % (78/79) for GSS-50. Collectively, the average percentage of the reproducibility of independent runs was 98.9 % for our tests. The discordant site was the same among all the samples, and a homopolymer error led to different INDEL lengths in each sample at chr2:47641559.

Concordance rate for SNP microarray platform

Next, variants generated using our approach were compared with the HapMap genotype data generated by SNP arrays as the gold standard. Five HapMap Japanese DNAs (NA18942, NA18945, NA18953, NA18959, and NA18974) were used to assess the accuracy of our method. Variants found using our approach were compared to the genotyped data generated in 1000 genomes projects obtained using an SNP array (ftp://ftp.1000genomes.ebi.ac.uk/vol1/ftp/release/20130502/supporting/hd_genotype_chip/broad_intensities/Omni25_genotypes_2141_samples.b37.v2.vcf.gz). In these samples, a total of 227 SNV sites were located within the target genes and were compared with the sequencing data. We correctly genotyped at least 224 of these 227 variant sites (98.7 %) among all the samples. Of the three variant sites that showed inconsistencies in any of the samples, one variant from NA18942 (G/A in chr2:190719499) was not available in the SNP array platform. The remaining two variants (chr5: 112082945 and chr5: 112180228) flanked erroneous homopolymer sites, which are known to produce artifacts in sequencing and variant calling. The concordance information for each of the samples is shown in Table 3, and all the comparable sites are shown in Supplementary Table S2.

Discussion

Here, we described the development of target enrichment and high-throughput sequencing for 20 genes implicated in familial colorectal, gastric, and related cancers and polyposis. In this study, we demonstrated that HaloPlex captured the targeted regions with a high efficiency (99.66 % for covered target regions, and 99.998 % for breadth of coverage), and that MiSeq could achieve a high accuracy (at least 98.7 % for the concordant rate with SNP arrays). Using this approach, we correctly identified 33/33 (100 %) confirmed alterations including SNV, small INDELs, and large deletions and an insertion in *APC, BMPR1A,*

Table 2 Point mutations, small insertions, and deletions identified

ID	Gene	Mutations	Chr	Start	End	Total reads	Variant reads
GSS-01	APC	NM_000038:exon16:c.3180_3184del:p.I1060fs	5	11,21,74,471	11,21,74,475	301	158
GSS-02	APC	NM_000038:exon11:c.1370delC:p.S457fs	5	11,21,57,650	11,21,57,650	696	336
GSS-08	APC	NM_000038:exon16:c.2804dupA:p.Y935_N936delinsX	5	11,21,74,094	11,21,74,094	298	153
GSS-09	APC	NM_000038:exon16:c.3429T>G:p.Y1143X	5	11,21,74,720	11,21,74,720	554	264
GSS-10	APC	NM_000038:exon16:c.4465_4466insGCCACAG: p.L1489fs	5	11,21,75,756	11,21,75,756	179	85
GSS-11	APC	NM_000038:exon12:c.1495C>T:p.R499X	5	11,21,62,891	11,21,62,891	629	299
GSS-13	APC	NM_000038:exon16:c.3921_3925del:p.I1307fs	5	11,21,75,212	11,21,75,216	410	199
GSS-19	APC	NM_000038:exon6:c.540_543del:p.L180fs	5	11,21,16,495	11,21,16,498	706	344
GSS-20	APC	NM_000038:exon12:c.1495_1496insTA:p.R499fs	5	11,21,62,891	11,21,62,891	788	380
GSS-21	APC	NM_000038:exon14:c.1690C>T:p.R564X	5	11,21,64,616	11,21,64,616	543	271
GSS-22	APC	NM_000038:exon10:c.994C>T:p.R332X	5	11,21,54,723	11,21,54,723	753	403
GSS-23	APC	NM_000038:exon16:c.2677G>T:p.E893X	5	11,21,73,968	11,21,73,968	318	150
GSS-24	APC	NM_000038:exon9:c.924_925delinsA:p.G309fs	5	11,21,51,281	11,21,51,282	359	197
GSS-25	APC	NM_000038:exon6:c.540_543del:p.L180fs	5	11,21,16,495	11,21,16,498	657	320
GSS-26	APC	NM_000038:exon16:c.2751delT:p.D917fs	5	11,21,74,042	11,21,74,042	293	141
GSS-32	APC	NM_000038:exon16:c.3133C>T:p.Q1045X	5	11,21,74,424	11,21,74,424	417	209
GSS-33	APC	NM_000038:exon16:c.2791_2794del:p.H931fs	5	11,21,74,082	11,21,74,085	293	129
GSS-14	MSH6	NM_000179:exon5:c.3254dupC:p.T1085fs	2	4,80,30,639	4,80,30,639	289	131
GSS-29	BMPR1A	NM_004329:exon10:c.1086_1087insCT:p.D362fs	10	8,86,79,146	8,86,79,146	219	50
GSS-49	MSH6	NM_000179:exon4:c.1806_1809del:p.S602fs	2	4,80,26,928	4,80,26,931	722	371
GSS-50	MLH1	NM_000249:exon3:c.209_211del:p.70_71del	3	3,70,42,447	3,70,42,449	627	309
GSS-51	MLH1	NM_000249:exon6:c.545 + 1G>C	3	3,70,50,397	3,70,50,397	503	156
GSS-59	MSH2	NM_000251:exon13:c.2142dupT:p.A714fs	2	4,77,03,641	4,77,03,641	327	143
GSS-64	PMS2	NM_000535:exon11:c.1572delA:p.P524fs	7	60,26,824	60,26,824	453	206
GSS-67	PMS2	NM_000535:exon8:c.861_864del:p.R287fs	7	60,35,204	60,35,207	505	228

EPCAM, MLH1, MSH2, MSH6, PMS2, and *SKT11*. We sometimes experienced difficulties in diagnosis based on the phenotypes and clinical features, including the number of polyps, the localization of polyps, the histological diagnosis, and the site of the occurrence of various extra-colonic cancers, among HGICS. Therefore, we proposed that a comprehensive analysis of 20 genes responsible for HGICS and investigated in this study might be useful for confirming a diagnosis. Consequently, our strategy might also be useful for the clinical management of HGICS, since the treatment and surveillance of polyps and cancer differs depending on the type of HGICS.

Our approach could correctly detect all large copy number changes (6 deletions and 1 duplication) that spanned multiple exons as well as an insertion located in a single exon. In addition, we simultaneously identified a frameshift mutation in exon 4 of *MSH6* and an insertion in the last exon of *MSH6* in GSS-49. Based on these findings, we estimated that our approach could identify several kinds of mutations/variants for multiple genes in a single patient simultaneously. These two variants, namely c.1806_1809del and c.4016_4068dup, found in GSS-49 were separated by ~7 kb fragment in the gene. Thus we could not determine whether these mutations located in cis or trans based on our sequence data. However, with regard to the clinical information of GSS-49, the patient suffered primary sigmoid colon cancer at the age of 47 years old and had no history of any caner prior to the discovery. Based on the clinical information, we could not find any phenotype of constitutional mismatch repair deficiency syndrome for this case. Compared with exome sequencing, target enrichment sequencing produced a higher coverage, thereby increasing the sensitivity of detecting all kinds of variations.

Since it takes a couple of weeks to run the HiSeq and the system requires sufficient numbers of samples to examine at a single time so as to maintain cost efficiency, improvements from the viewpoint of timesaving at a reasonable cost are necessary. The HaloPlex and other target enrichment platforms enable laborious PCR experiments for each exon to be avoided. The combination of HaloPlex and MiSeq could generate sequencing results within a week. This fast turnover and cost reduction are ideal specifications for the small clinical laboratory setting.

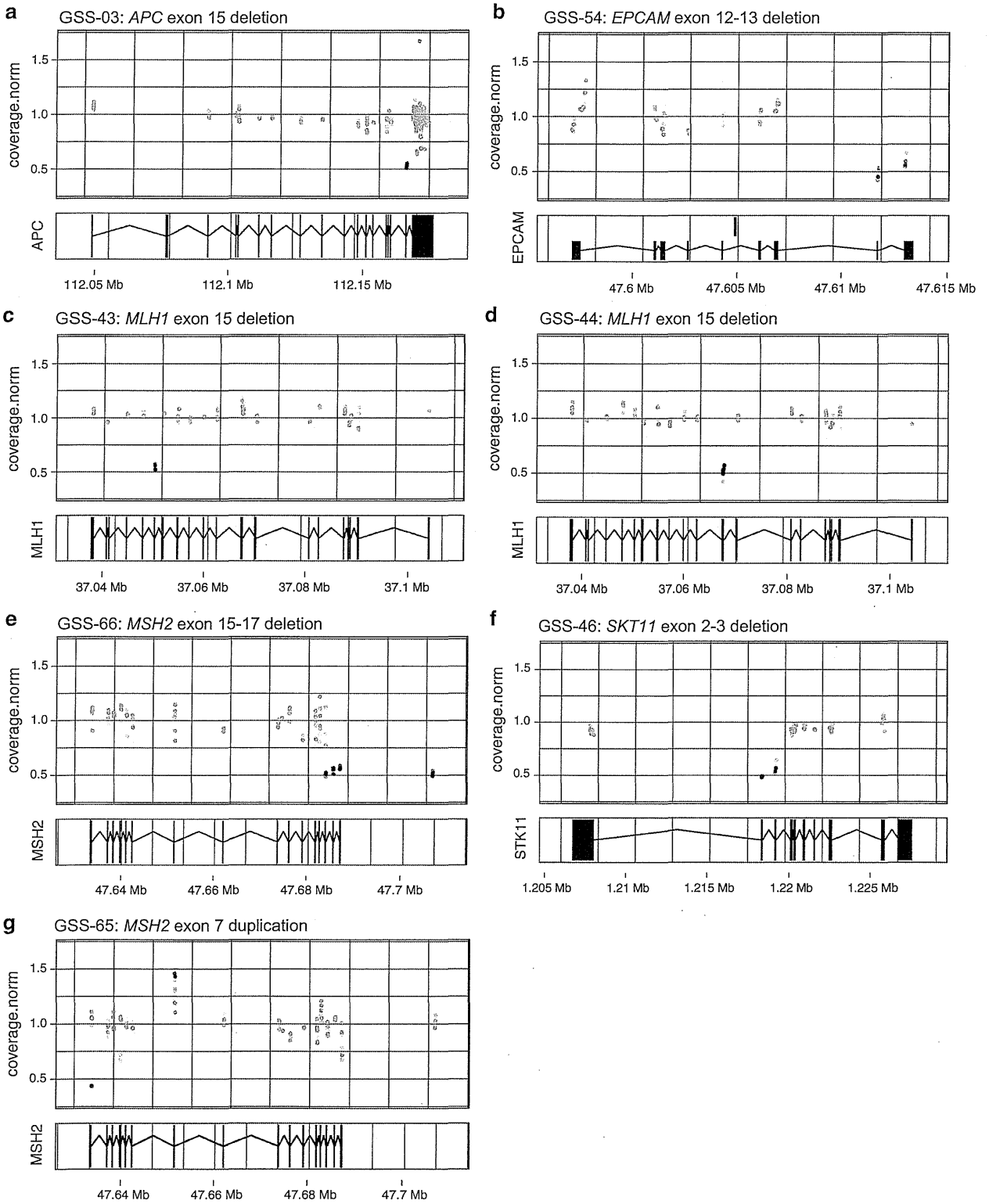

Fig. 2 Exonic deletions and a duplication in target genes. **a**–**e** exonic deletions of *APC*, *EPCAM*, *MLH1*, *MSH2*, and *STK11* genes. **g** exonic duplication of *MSH2* gene depth of coverage is normalized across all samples in the same run. Normalized depth ratios of each base pair are represented in *gray*. Depth of coverage deviating from the median of all samples are colored in *red* or *blue* (*red* for exonic deletions, and *blue* for duplications). *Black vertical lines* indicate exons. *Horizontal lines* indicate intervening introns. Genomic coordinates shown on the x-axis are hg19. (Color figure online)

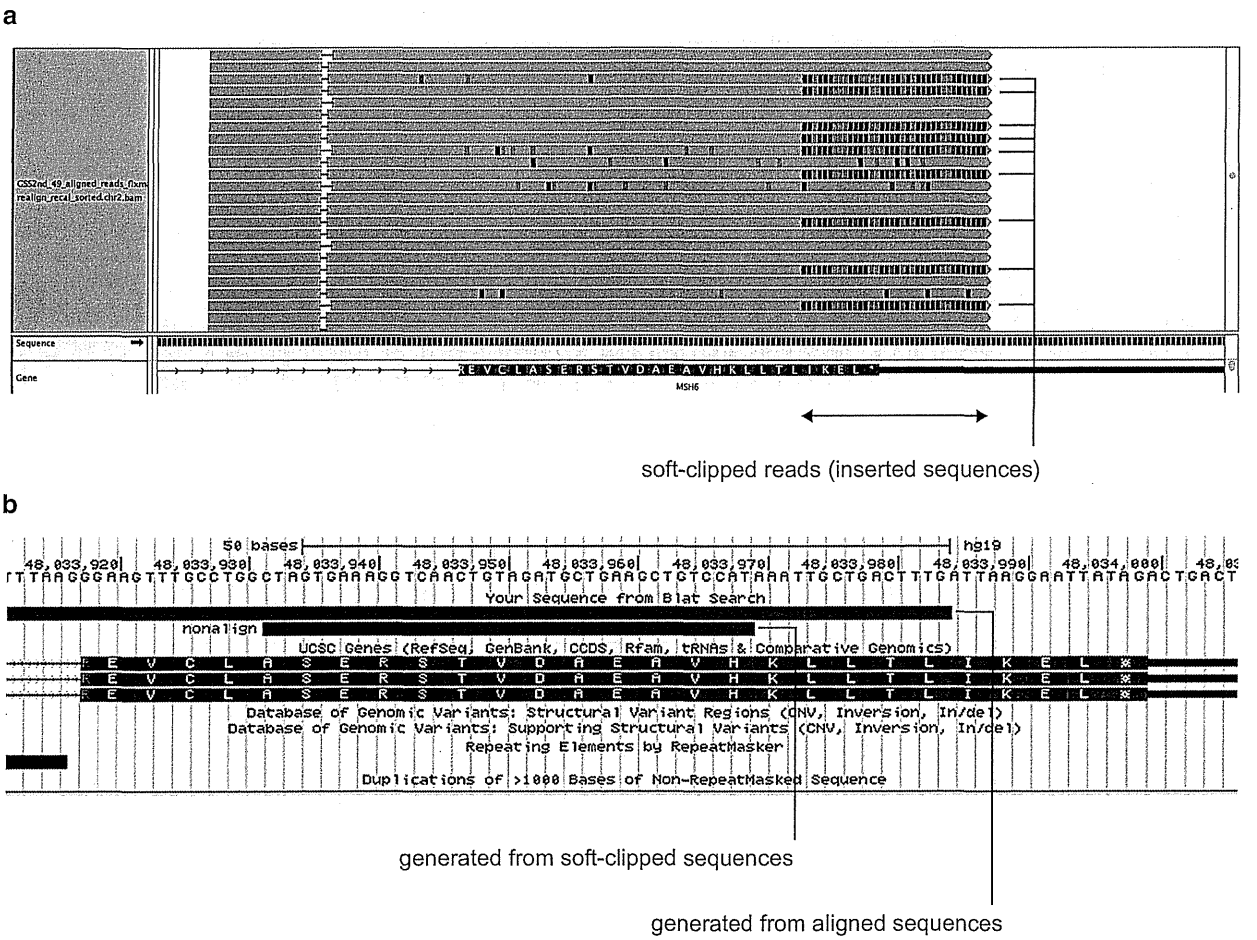

Fig. 3 A large insertion in identified by soft-clipped reads analysis. Integrative genomics viewer screen shot of soft-clipped reads in the last exon of *MSH6*. About half of the aligned reads of GSS-49 specifically have abnormal sequences **a**. UCSC Genome browser screen shot of BLAT analysis with the assembled read generated from soft-clipped reads of GSS-49. The soft-clipped sequences completely matched with upstream genomic sequences of the *left* breakpoint (**b**)

Table 3 Concordance between SNP array and our targeted sequencing

	NA18942	NA18945	NA18953	NA18959	NA18974
Sites detected by SNP array	227	227	227	227	227
Sites detected by sequence	226	227	227	227	227
Concordant sites	224	227	225	225	225
Concordant rate (%)	98.7	100	99.1	99.1	99.1

High-throughput sequencing-based testing can overcome some of the limitations of low-throughput methods, but this approach has some drawbacks: (1) because of the short read length, such as 150 bp, high-throughput methods are less capable of determining the complete sequences of structure variations than Sanger sequencing technology, and (2) our current approach cannot distinguish somatic mutations with low mutation loads. As an example of the former drawback, in this study, we estimated the length of an inserted sequence in GSS-49 to be 38 bp. However, Sanger sequence validation revealed the length to be 53 bp (c.4016_4068dup). This discrepancy arose because the 150-bp sequence length was too short to reveal the full inserted sequence. This drawback can be overcome if longer sequence reads are used, such as 300-bp paired sequence kits. The reason for the latter drawback is that DNA fragments are generated using restriction enzymes in the HaloPlex platform; therefore, this platform cannot

distinguish PCR-duplicated clones in the library. For this reason, our current approach is unsuitable for detecting low-frequency somatic mutations. However, the recently announced HaloPlexHS, which consists of a HaploPlex with molecular barcodes, can resolve such sequencing problems and can be used to detect low-frequency somatic/germline mutations accurately in subclonal cell populations [24]. Using this new product, we hope to apply our prototype to cancer specimens.

High-throughput sequencing technology is rapidly changing the landscape of genetic testing. At least 2 recent studies have evaluated target capture and high-throughput sequencing for Lynch and polyposis syndromes [5, 25]. In these studies, target capturing and sequencing were achieved using the NimbleGen custom array/HiSeq 2000 and the Agilent SureSelect/HiSeq 2000. Both studies showed impressive performances for identifying mutations. However, they also involved a long turnaround time as a limitation of the assays. Our approach could enable runs with a smaller sample size and with a short turnaround time. In addition, the longer reads of MiSeq enable better performances in terms of determining the full sequences of structure variations, such as long insertions.

Genetic testing methods based on hybridization capture and high-throughput sequencing are becoming widely applied for genetic testing purposes, including cancers. The platforms used in this study have some advantages. Our approach is designed to enable the use of a smaller sample size, to provide a more clinically oriented instrument, and to achieve a faster turnaround time. The approach is capable of sequencing 20 target genes at once and can simultaneously detect all types of variations, including structure variations, because of its use of longer sequence reads. Our results suggest that our approach is sufficient for the rapid screening of known causative gene mutations of inherited colon cancers, such as familial adenomatous polyposis, Lynch syndrome, Peutz–Jeghers syndrome, and Juvenile polyposis syndrome.

Funding This study was supported in part by a grant-in-aid for the Support Project of the Strategic Research Center in Private Universities from the Ministry of Education, Culture, Sports, Science and Technology (MEXT) of Japan awarded to the Saitama Medical University Research Center for Genomic Medicine.

Compliance with ethical standards

Conflict of interest None of the authors have conflict of interest.

References

1. Syngal S, Brand RE, Church JM, Giardiello FM, Hampel HL, Burt RW, American College of Gastroenterology (2015) ACG clinical guideline: genetic testing and management of hereditary gastrointestinal cancer syndromes. Am J Gastroenterol 110:223–262. doi:10.1038/ajg.2014.435
2. Oliveira C, Pinheiro H, Figueiredo J, Seruca R (2015) Familial gastric cancer: genetic susceptibility, pathology, and implications for management. The Lancet 16:e60–e70. doi:10.1016/S1470-2045(14)71016-2
3. Palles C, Cazier J-B, Howarth KM, Domingo E, Jones AM, Broderick P, Kemp Z, Spain SL, Guarino E, Guarino Almeida E, Salguero I, Sherborne A, Chubb D, Carvajal-Carmona LG, Ma Y, Kaur K, Dobbins S, Barclay E, Gorman M, Martin L, Kovac MB, Humphray S, CORGI Consortium, WGS500 Consortium, Lucassen A, Holmes CC, Bentley D, Donnelly P, Taylor J, Petridis C, Roylance R, Sawyer EJ, Kerr DJ, Clark S, Grimes J, Kearsey SE, Thomas HJW, McVean G, Houlston RS, Tomlinson I (2013) Germline mutations affecting the proofreading domains of POLE and POLD1 predispose to colorectal adenomas and carcinomas. Nat Publ Group 45:136–144. doi:10.1038/ng.2503
4. Aretz S (2010) The differential diagnosis and surveillance of hereditary gastrointestinal polyposis syndromes. Deutsch Arzteblatt Int 107(10):163
5. Pritchard CC, Smith C, Salipante SJ, Lee MK, Thornton AM, Nord AS, Gulden C, Kupfer SS, Swisher EM, Bennett RL, Novetsky AP, Jarvik GP, Olopade OI, Goodfellow PJ, King M-C, Tait JF, Walsh T (2012) ColoSeq provides comprehensive lynch and polyposis syndrome mutational analysis using massively parallel sequencing. J Mol Diagn 14:357–366. doi:10.1016/j.jmoldx.2012.03.002
6. Yurgelun MB (2015) Next-zfor hereditary colorectal cancer risk assessment. J Clin Oncol 33:388–393. doi:10.1200/JCO.2014.58.9895
7. Cragun D, Radford C, Dolinsky JS, Caldwell M, Chao E, Pal T (2014) Panel-based testing for inherited colorectal cancer: a descriptive study of clinical testing performed by a US laboratory. Clin Genet 86:510–520. doi:10.1111/cge.12359
8. Yurgelun MB, Allen B, Kaldate RR, Bowles KR (2015) Identification of a variety of mutations in cancer predisposition genes in patients with suspected lynch syndrome. Gastroenterology 149(604–613):e620. doi:10.1053/j.gastro.2015.05.006
9. Gréen A, Gréen H, Rehnberg M, Svensson A, Gunnarsson C, Jonasson J (2015) Assessment of HaloPlex amplification for sequence capture and massively parallel sequencing of arrhythmogenic right ventricular cardiomyopathy-associated genes. J Mol Diagn 17:31–42. doi:10.1016/j.jmoldx.2014.09.006
10. Mertes F, Elsharawy A, Sauer S, van Helvoort JMLM, van der Zaag PJ, Franke A, Nilsson M, Lehrach H, Brookes AJ (2011) Targeted enrichment of genomic DNA regions for next-generation sequencing. Brief Funct Genom 10:33–386. doi:10.1093/bfgp/elr033
11. Bolger AM, Lohse M, Usadel B (2014) Trimmomatic: a flexible trimmer for Illumina sequence data. Bioinformatics 30:2114–2120. doi:10.1093/bioinformatics/btu170 **(Oxford, England)**
12. Li H, Durbin R (2009) Fast and accurate short read alignment with Burrows–Wheeler transform. Bioinformatics 25:1754–1760. doi:10.1093/bioinformatics/btp324 **(Oxford, England)**
13. Li H, Handsaker B, Wysoker A, Fennell T, Ruan J, Homer N, Marth G, Abecasis G, Durbin R, 1000 Genome Project Data Processing Subgroup (2009) The sequence alignment/map format and SAMtools. Bioinformatics 25:2078–2079. doi:10.1093/bioinformatics/btp352 **(Oxford, England)**
14. McKenna A, Hanna M, Banks E, Sivachenko A, Cibulskis K, Kernytsky A, Garimella K, Altshuler D, Gabriel S, Daly M, DePristo MA (2010) The genome analysis toolkit: a MapReduce framework for analyzing next-generation DNA sequencing data. Genome Res 20:1297–1303. doi:10.1101/gr.107524.110

15. Wang K, Li M, Hakonarson H (2010) ANNOVAR: functional annotation of genetic variants from high-throughput sequencing data. Nucleic Acids Res 38:e164. doi:10.1093/nar/gkq603
16. International HapMap 3 Consortium, Altshuler DM, Gibbs RA, Peltonen L, Dermitzakis E, Schaffner SF, Yu F, Bonnen PE, de Bakker PIW, Deloukas P, Gabriel SB, Gwilliam R, Hunt S, Inouye M, Jia X, Palotie A, Parkin M, Whittaker P, Chang K, Hawes A, Lewis LR, Ren Y, Wheeler D, Muzny DM, Barnes C, Darvishi K, Hurles M, Korn JM, Kristiansson K, Lee C, McCarrol SA, Nemesh J, Keinan A, Montgomery SB, Pollack S, Price AL, Soranzo N, Gonzaga-Jauregui C, Anttila V, Brodeur W, Daly MJ, Leslie S, Mcvean G, Moutsianas L, Nguyen H, Zhang Q, Ghori MJR, Mcginnis R, McLaren W, Takeuchi F, Grossman SR, Shlyakhter I, Hostetter EB, Sabeti PC, Adebamowo CA, Foster MW, Gordon DR, Licinio J, Manca MC, Marshall PA, Matsuda I, Ngare D, Wang VO, Reddy D, Rotimi CN, Royal CD, Sharp RR, Zeng C, Brooks LD, McEwen JE (2010) Integrating common and rare genetic variation in diverse human populations. Nature 467:52–58. doi:10.1038/nature09298
17. Thompson BA, Spurdle AB, Plazzer J-P, Greenblatt MS, Akagi K, Al-Mulla F, Bapat B, Bernstein I, Capellá G, den Dunnen JT, du Sart D, Fabre A, Farrell MP, Farrington SM, Frayling IM, Frébourg T, Goldgar DE, Heinen CD, Holinski-Feder E, Kohonen-Corish M, Robinson KL, Leung SY, Martins A, Moller P, Morak M, Nystrom M, Peltomaki P, Pineda M, Qi M, Ramesar R, Rasmussen LJ, Royer-Pokora B, Scott RJ, Sijmons R, Tavtigian SV, Tops CM, Weber T, Wijnen J, Woods MO, Macrae F, Genuardi M (2013) Application of a 5-tiered scheme for standardized classification of 2,360 unique mismatch repair gene variants in the InSiGHT locus-specific database. Nat Publ Group 46:107–115. doi:10.1038/ng.2854
18. Stenson PD, Mort M, Ball EV, Shaw K, Phillips A, Cooper DN (2014) The human gene mutation database: building a comprehensive mutation repository for clinical and molecular genetics, diagnostic testing and personalized genomic medicine. Hum Genet 133:1–9. doi:10.1007/s00439-013-1358-4
19. Quinlan AR, Hall IM (2010) BEDTools: a flexible suite of utilities for comparing genomic features. Bioinformatics 26:841–842. doi:10.1093/bioinformatics/btq033 **(Oxford, England)**
20. Yin T, Cook D, Lawrence M (2012) ggbio: an R package for extending the grammar of graphics for genomic data. Genome Biol 13(8):R77
21. Wang J, Mullighan CG, Easton J, Roberts S, Heatley SL, Ma J, Rusch MC, Chen K, Harris CC, Ding L, Holmfeldt L, Payne-Turner D, Fan X, Wei L, Zhao D, Obenauer JC, Naeve C, Mardis ER, Wilson RK, Downing JR, Zhang J (2011) CREST maps somatic structural variation in cancer genomes with base-pair resolution. Nat Meth 8:652–654. doi:10.1038/nmeth.1628
22. Kent WJ, Sugnet CW, Furey TS, Roskin KM, Pringle TH, Zahler AM, Haussler D (2002) The human genome browser at UCSC. Genome Res 12:996–1006. doi:10.1101/gr.229102
23. Robinson JT, Thorvaldsdóttir H, Winckler W, Guttman M, Lander ES, Getz G, Mesirov JP (2011) Integrative genomics viewer. Nat Biotechnol 29:24–26. doi:10.1038/nbt.1754
24. Salo-Mullen EE, Shia J, Brownell I, Allen P, Girotra M, Robson ME, Offit K, Guillem JG, Markowitz AJ, Stadler ZK (2014) Mosaic partial deletion of the PTEN gene in a patient with Cowden syndrome. Fam Cancer 13:459–467. doi:10.1007/s10689-014-9709-4
25. Guan Y, Hu H, Peng Y, Gong Y, Yi Y, Shao L, Liu T, Li G, Wang R, Dai P, Bignon Y-J, Xiao Z, Yang L, Mu F, Xiao L, Xie Z, Yan W, Xu N, Zhou D, Yi X (2014) Detection of inherited mutations for hereditary cancer using target enrichment and next generation sequencing. Fam Cancer. doi:10.1007/s10689-014-9749-9

Computer-aided diagnosis of colorectal polyp histology by using a real-time image recognition system and narrow-band imaging magnifying colonoscopy

Yoko Kominami, MD,[1] Shigeto Yoshida, MD, PhD,[2] Shinji Tanaka, MD, PhD,[2] Yoji Sanomura, MD, PhD,[2] Tsubasa Hirakawa, ME,[3] Bisser Raytchev, PhD,[3] Toru Tamaki, PhD,[3] Tetsusi Koide, PhD,[4] Kazufumi Kaneda, PhD,[3] Kazuaki Chayama, MD, PhD[1]

Hiroshima, Japan

Background and Aims: It is necessary to establish cost-effective examinations and treatments for diminutive colorectal tumors that consider the treatment risk and surveillance interval after treatment. The Preservation and Incorporation of Valuable Endoscopic Innovations (PIVI) committee of the American Society for Gastrointestinal Endoscopy published a statement recommending the establishment of endoscopic techniques that practice the resect and discard strategy. The aims of this study were to evaluate whether our newly developed real-time image recognition system can predict histologic diagnoses of colorectal lesions depicted on narrow-band imaging and to satisfy some problems with the PIVI recommendations.

Methods: We enrolled 41 patients who had undergone endoscopic resection of 118 colorectal lesions (45 non-neoplastic lesions and 73 neoplastic lesions). We compared the results of real-time image recognition system analysis with that of narrow-band imaging diagnosis and evaluated the correlation between image analysis and the pathological results.

Results: Concordance between the endoscopic diagnosis and diagnosis by a real-time image recognition system with a support vector machine output value was 97.5% (115/118). Accuracy between the histologic findings of diminutive colorectal lesions (polyps) and diagnosis by a real-time image recognition system with a support vector machine output value was 93.2% (sensitivity, 93.0%; specificity, 93.3%; positive predictive value (PPV), 93.0%; and negative predictive value, 93.3%).

Conclusions: Although further investigation is necessary to establish our computer-aided diagnosis system, this real-time image recognition system may satisfy the PIVI recommendations and be useful for predicting the histology of colorectal tumors.

Colorectal tumors are among the most common tumors worldwide. Most adenomas are considered premalignant lesions,[1] and the number of adenomas is a good determining factor for predicting the long-term risk of advanced neoplasia.[2-4] A recent report showed that colonoscopy and sigmoidoscopy are associated with a reduced incidence of cancer.[5] It is necessary to establish cost-effective examinations and treatments for small colorectal tumors that consider the treatment risk and surveillance interval after treatment. The Preservation and Incorporation of Valuable Endoscopic Innovations (PIVI) committee of the American Society for Gastrointestinal Endoscopy published a statement on establishing endoscopic techniques that practice the resect and discard strategy.[6] Therefore, it is necessary to provide endoscopic treatment that is consistent with the PIVI recommendations. Recently, combining the narrow-band imaging (NBI) system and magnifying endoscopy allows simple and clear visualization of the microscopic structures of the superficial mucosa and its capillary patterns.[7] NBI magnifying endoscopy may be useful for providing a precise endoscopic diagnosis of a histological diagnosis. Various NBI classifications such as the Hiroshima classification,[8] which correlates with the histologic

Abbreviations: NBI, narrow-band imaging; NPV, negative predictive value; PIVI, Preservation and Incorporation of Valuable Endoscopic Innovations; PPV, positive predictive value; ROI, region of interest; SIFT, scale-invariant feature transform; SVM, support vector machine.

DISCLOSURE: *All authors disclosed no financial relationships relevant to this article.*

0016-5107/$36.00
http://dx.doi.org/10.1016/j.gie.2015.08.004

Received March 25, 2015. Accepted August 2, 2015.

Current affiliations: Departments of Gastroenterology and Metabolism (1) and Endoscopy and Medicine (2), Graduate School of Biomedical and Health Science, Department of Information Engineering, Graduate School of Engineering (3), Research Institute for Nanodevice and Bio Systems (4), Hiroshima University, Hiroshima, Japan.

Reprint requests: Shigeto Yoshida, MD, PhD, Department of Endoscopy and Medicine, Hiroshima University, 1-2-3 Kasumi, Minami-ku, Hiroshima 734-8551, Japan.

features, is clinically useful for determining treatment options for colorectal tumors.[9-11] However, an NBI-based diagnosis requires training and experience, and an objective diagnosis is necessary. Therefore, we are developing a computerized system[12] that provides a more objective diagnosis, which allows nonexpert endoscopists to achieve a high diagnostic accuracy. We report an improved software program that can evaluate colorectal lesions using real-time colonoscopy. We evaluated the use of this real-time image recognition system by using NBI magnifying colonoscopy with a support vector machine (SVM) output value to satisfy some problems in the PIVI recommendations.

MATERIALS AND METHODS

Specimen preparation and instruments

We examined 118 lesions (88 lesions, ≤5 mm; 12 lesions, 6–9 mm; and 18 lesions, ≥10 mm) obtained from 41 patients (29 male and 12 female, 67.3 ± 7.9 years of age) who underwent EMR, endoscopic submucosal dissection, and biopsy for colorectal lesions. The patients were treated at Hiroshima University Hospital between October 2014 and March 2015. Patients with sessile serrated adenomas and traditional serrated adenomas were excluded. Pathologic examinations were performed by using hematoxylin and eosin–stained sections by a single GI pathologist blinded to the endoscopic and real-time image recognition system diagnosis. Pathology was used as the criterion standard.

The intervals for postpolypectomy surveillance that would be recommended by using the real-time image recognition system instead of endoscopic predictions of histology were compared with those that would be recommended by using the pathologic findings. The recommended follow-up intervals from the U.S. Multi-Society Task Force and American Cancer Society guideline[13] were used.

The study received full approval from the Ethics Committee of Hiroshima University, was performed at the Department of Endoscopy and Medicine, Hiroshima University, Hiroshima, Japan, and was conducted in accordance with the guidelines of the Declaration of Helsinki. Patients and/or their family members provided informed consent for the endoscopic examination and pathologic study of resected specimens.

Instruments used in this study included a magnifying videoscope system (CF-H260AZI; Olympus Optical Co, Ltd, Tokyo, Japan), which provides a magnifying power of up to 80× (optical magnification), and the EVIS LUCERA ELITE Video System Center CV-290 (Olympus Medical Systems, Tokyo, Japan). Lesions detected by conventional colonoscopy were observed by using NBI at the optical maximum magnification, and the obtained NBI magnifying images were analyzed in real time by using our newly developed image recognition system.

COLONOSCOPY PROCEDURE AND NBI CHARACTERIZATION OF THE LESIONS

An endoscopist with 6 years of colonoscopy experience focused images at the optical maximum magnification, analyzed the NBI magnifying images in focus without motion blur of the colorectal lesions in real time, and obtained still NBI magnifying colorectal lesion images. Another endoscopist with more than 20 years of colonoscopy experience who was blinded to the histologic findings and real-time image recognition system findings classified the still NBI magnifying images as type A or type B–C with a high or low confidence prediction according to the Hiroshima classification system after the procedure. In our study, high- and low-confidence predictions were made in 95.8% (113/118) and 4.2% (5/118) of lesions, respectively. The Hiroshima classification divides microvessels and the surface structure in a narrow-band image into types A, B, or C. This classification system reportedly correlates with histological diagnoses.[8] Type A corresponds to nonneoplastic lesions, whereas type B–C corresponds to neoplastic lesions.

Real-time image recognition system

For the quantitative analysis of colorectal lesions, we developed a custom software program that can display features of endoscopic images and quantify each image according to the corresponding features on the training image. To develop the image recognition system, we prepared a set of 2247 cutout training images (504 type A and 1743 types B–C3 images) from 1262 colorectal lesions that were collected before this study at the optical maximum NBI magnification in the same manner as in this study at Hiroshima University Hospital. The set did not include images that were considered unsuitable for evaluation (exclusion criteria were out-of-focus images, motion blurred images, and those with halation). We used a bag-of-features representation in which an image is represented by a histogram of visual words that are produced by a hierarchical k-means clustering of scale-invariant feature transform (SIFT) descriptors as local features. In this study, SIFT descriptors, in which each descriptor is a 128-dimensional vector, were computed at points on a regular grid of 5 pixels with dense spacing and also at 2 different scales (5 and 7 pixels) of local patches, which were centered at each grid point. A regular grid was used because the texture of each narrow-band image filled the whole image. An SVM with a linear kernel was used as the classifier (Fig. 1).

By using an SVM and logistic regression, we calculated the SVM output value for the real-time recognition system. The simple logistic function was defined by the following formula: $P(t) = 1/(1 + e^{-t})$, where P denotes the SVM output value, t denotes the distance from the boundary line for type A or B–C, and e is the exponential function.

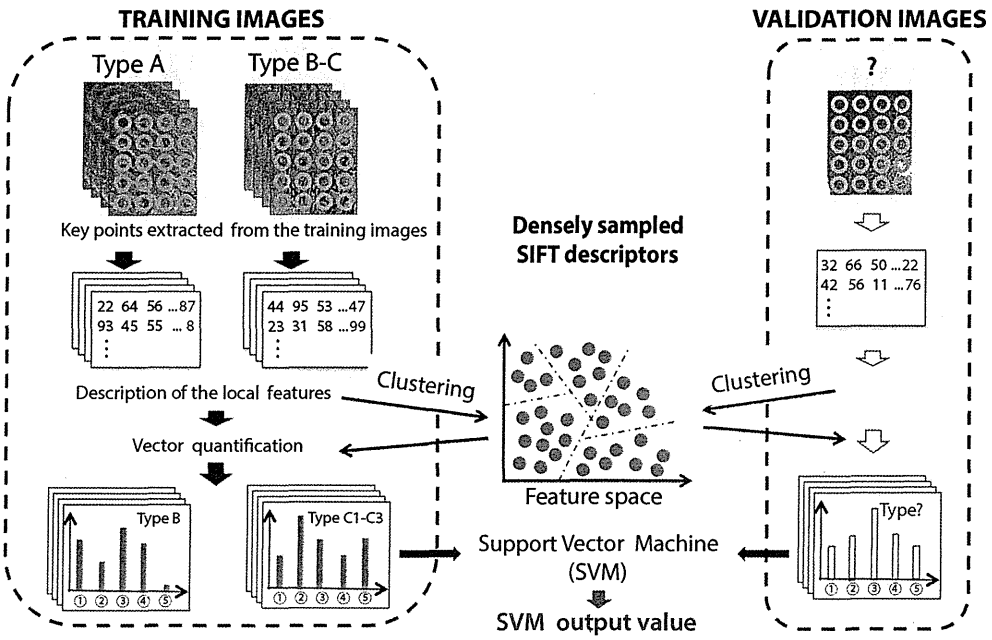

Figure 1. Flow diagram of the quantification of a computerized system for analyzing narrow-band images. The system uses densely sampled scale-invariant feature transform (SIFT) descriptors in a bag-of-features framework followed by a support vector machine (SVM) classifier.

Our real-time recognition system analyzed the region of interest (ROI) (the center of the endoscopic image: 200 × 200 pixels) of the NBI videoendoscopic image (1920 × 1080 pixels), and the SVM output values were provided on the screen in real time (Fig. 2). The frame rate of this system is 20 frame/s, and this system analyzes frame-by-frame with high-quality images. The cutoff value of this SVM output value was 0.5. The SVM output values were defined as follows: nonneoplastic lesion, ≤0.5 (0–0.5) and neoplastic lesion, >0.5 (0.5–1.0).

Colorectal lesion description

The size, location, and morphology were documented for each lesion. The size was estimated by comparing the lesion size with the span of the open biopsy forceps. Each lesion was assigned to one of the bowel segments. The Paris classification system for superficial neoplastic lesions in the digestive tract was used to define the lesion morphology (Table 1).[14]

Sample size

In our study, approximately 95% of the distribution's probability lay within 2 SDs of the mean. According to the PIVI recommendations, a histologic assessment of lesions (polyps) ≤5 mm should provide a 90% negative predictive value (NPV) for adenomatous histology. Thus, a lower confidence level must be >90%. A confidence level of 95% and a margin of error of ±5% indicated an approximate sample size of 76 to evaluate the accuracy of the real-time image recognition system. We collected samples regardless of the size and acquired the diminutive colorectal polyps for 76 lesions. We examined 88 diminutive colorectal lesions according to the PIVI criteria.

Statistical analysis

Values are reported as mean (SD). Differences in the SVM output values between the nonneoplastic and neoplastic lesions were analyzed by using the Mann-Whitney U test.

In the histologic results, agreement between the results of the real-time image recognition system and the endoscopic diagnosis was tested by using the κ statistic.

All statistical analyses were performed in the R environment for statistical analyses (R Project, Vienna, Austria), and $P < .05$ was considered statistically significant.

RESULTS

At colonoscopy, 118 lesions were detected and retrieved for histologic analysis. The endoscopic and histologic characteristics of the lesions are presented in Table 1.

NBI characterization was feasible in all retrieved lesions by using the Hiroshima classification system. Overall, 45 lesions (38.1%) were nonneoplastic (hyperplastic polyps) on histological evaluation, whereas 73 (61.9%) were neoplastic (66 adenomas, 7 adenocarcinomas with intramucosal invasion).

Of the diminutive colorectal lesions (polyps), 45 (51.1%) were nonneoplastic, and 43 (48.9%) were neoplastic (only adenomas).

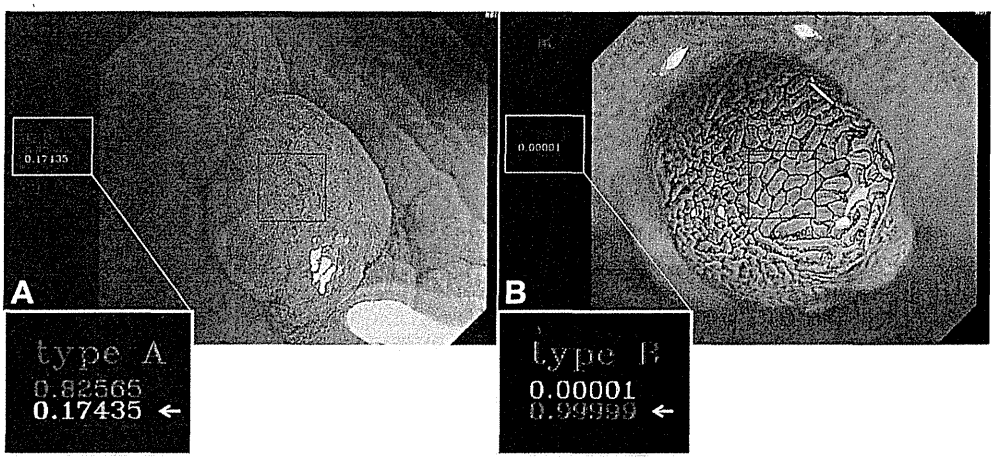

Figure 2. The computer-aided diagnosis system recognizes and classifies colorectal lesions by using narrow-band imaging magnifying colonoscopy in real time. The support vector machine output value in the region of interest (ROI) (*red square*) is shown on the second line of the left numerical value (*arrows*), and the classification of ROI is shown on the left of the screen (*yellow square*). **(A)** The real-time image recognition system analysis of a nonneoplastic lesion. **(B)** The real-time image recognition system analysis of a neoplastic lesion.

TABLE 1. Characteristics of the lesions detected in the study population

	≤5 mm	6–9 mm	≥10 mm	Total, no. (%)
Location				
Rectum	32 (36.4)	1 (8.3)	1 (5.6)	34 (28.8)
S/C	22 (25.0)	7 (58.4)	5 (27.7)	34 (28.8)
D/C	4 (4.5)	1 (8.3)	0	5 (4.2)
T/C	5 (5.7)	1 (8.3)	3 (16.7)	9 (7.7)
A/C	21 (23.9)	2 (16.7)	6 (33.3)	29 (24.6)
Cecum	4 (4.5)	0	3 (16.7)	7 (5.9)
Hiroshima classification				
Type A	42 (47.7)	0	0	42 (35.6)
Type B–C	46 (52.3)	12 (100)	18 (100)	76 (64.4)
Shape (Paris classification)				
Is	83 (94.3)	8 (66.7)	7 (38.9)	98 (83.0)
Isp	0	1 (8.3)	3 (16.7)	4 (3.4)
IIa	5 (5.7)	3 (25.0)	8 (44.4)	16 (13.6)
Histology				
Nonneoplastic lesion	45 (51.1)	0	0	45 (38.1)
Neoplastic lesion	43 (48.9)	12 (100)	18 (100)	73 (61.9)

The data are limited to the 118 retrieved polyps.
S/C, Sigmoid colon; *D/C*, descending colon; *T/C*, transverse colon; *A/C*, ascending colon.

Utility of the real-time image recognition system

The SMV output value of neoplastic lesions was significantly higher than that of nonneoplastic lesions ($P = 3.0 \times 10^{-16}$) (Fig. 3).

In our study, the cutoff value of the SVM output value was 0.50. By using this cutoff value, the accuracy calculated for evaluating concordance between diagnosis by a real-time image recognition system and the histologic findings

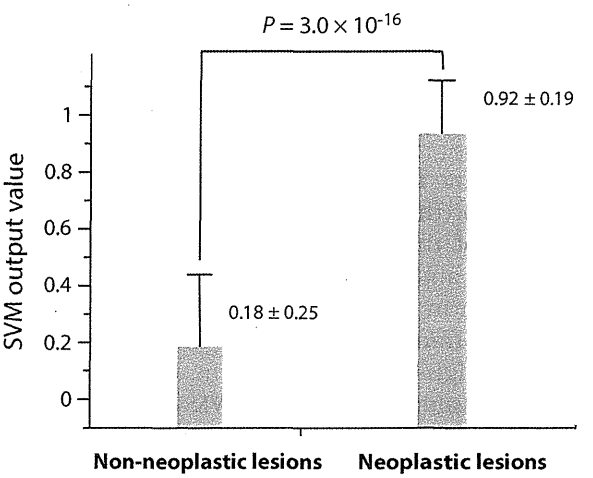

Figure 3. Support vector machine (SVM) output values for the images of nonneoplastic and neoplastic lesions ($P = 3.0 \times 10^{-16}$, Mann-Whitney *U* test).

was 94.9% (112/118) (sensitivity, 95.9%; specificity, 93.3%; PPV, 95.9%; and NPV, 93.3%) (Table 2). Further, we evaluated that concordance between the endoscopic diagnosis and diagnosis by a real-time image recognition system by using the SVM output value was 97.5% (115/118); the κ value between them was 0.95, and the agreement was excellent (Table 3). Concordance between the endoscopic diagnosis for the diminutive colorectal polyps and diagnosis by the real-time image recognition system by using the SVM output value was 96.6% (85/88); the κ value between them was 0.93, and the agreement was excellent (Table 4).

Agreement of the postpolypectomy surveillance intervals

Recommendations for follow-up colonoscopy based on pathology and the real-time image recognition system

TABLE 2. Relationship between the histologic findings and diagnosis by real-time image recognition system by using a support vector machine output value

Diagnosis by real-time image recognition system	Histologic findings, no. (%)	
	Nonneoplastic lesions	Neoplastic lesions
≤0.5	42 (93.3)	3 (4.1)
>0.5	3 (6.7)	70 (95.9)
Total	45 (100)	73 (100)

Accuracy, 94.9% (112/118); sensitivity, 95.9%; and specificity, 93.3%; positive predictive value/negative predictive value: 95.9%/93.3%.

TABLE 3. Relationship between the endoscopic diagnosis and diagnosis by real-time image recognition system by using a support vector machine output value

Diagnosis by real-time image recognition system	Endoscopic diagnosis, no. (%)	
	Type A	Type B–C3
≤0.5	42 (100)	3 (3.9)
>0.5	0 (0)	73 (96.1)
Total	42 (100)	76 (100)

κ statistic, 0.95 (excellent agreement); 95% confidence interval, 0.89–1.00. The concordance rate between the diagnosis by image recognition system and by endoscopists was 97.5% (115/118).

TABLE 4. Relationship between the endoscopic diagnosis for diminutive polyps (<5 mm) and diagnosis by real-time image recognition system using a support vector machine output value

Diagnosis by real-time image recognition system	Endoscopic diagnosis, no. (%)	
	Type A	Type B–C3
≤0.5	42 (100)	3 (6.5)
>0.5	0 (0)	43 (93.5)
Total	42 (100)	46 (100)

κ statistic, 0.93 (excellent agreement); 95% confidence interval, 0.86–1.00. The concordance rate between the diagnosis by image recognition system and by endoscopists was 96.6% (85/88).

TABLE 5. Relationship between the histologic findings of diminutive colorectal lesions (polyps) and diagnosis by real-time image recognition system by using a support vector machine output value

Diagnosis by real-time image recognition system	Histologic findings, no. (%)	
	Nonneoplastic lesions	Neoplastic lesions
≤0.5	42 (93.3)	3 (7.0)
>0.5	3 (6.7)	40 (93.0)
Total	45 (100)	43 (100)

Accuracy, 93.2% (82/88); sensitivity, 93.0%; and specificity, 93.3%; positive predictive value/negative predictive value: 93.0%/93.3%.

prediction of pathology were identical for 38 of 41 patients (92.7%).

NPV for the adenomatous histology of lesions (polyps) <5 mm

We evaluated diminutive colorectal lesions (polyps) and whether our system satisfied the PIVI recommendations. Accuracy between the histologic findings of diminutive colorectal lesions and the diagnosis by a real-time image recognition system by using the SVM output value was 93.2% (82/88) (sensitivity, 93.0%; specificity, 93.3%; PPV, 93.0%; and NPV, 93.3%) (Table 5).

DISCUSSION

A certain type of polyp known as an adenoma may have a higher risk of becoming cancerous. Therefore, elimination of a colon adenoma is an effective strategy for preventing the development of colon cancer. The current paradigm for diminutive polyp management (polyps ≤5 mm) is resection and pathologic evaluation. Pathology (adenoma vs hyperplastic) after removal is used to guide the postpolypectomy surveillance interval. This observation has generated interest in developing endoscopic imaging technologies that can serve as alternatives to the pathologist's examination of diminutive polyps and will be less expensive than histologic evaluations. The American Society for Gastrointestinal Endoscopy has recommended minimum performance thresholds for imaging technologies regarding clinically relevant endpoints.[15]

Recently, the qualitative diagnostic ability for colorectal tumors has progressed drastically; however, the accuracy of precise examinations is largely influenced by operator skill and experience.[16,17]

A recent study revealed that a high-confidence prediction of histology for polyps ≤5 mm appears sufficiently accurate for avoiding a postpolypectomy histologic examination of resected lesions and allows rectosigmoid hyperplastic polyps to be left in place without resection. Also, only experienced endoscopists participated in this study.[18] A current study evaluated real-time optical biopsy analysis of polyps with NBI by community-based gastroenterologists, and only 25% of gastroenterologists assessed polyps with >90% accuracy. The NPV for identifying adenomas, not the surveillance interval agreement, met the PIVI recommendations for optical biopsy.[19] Thus, we are developing a computer-aided diagnosis system that will provide a more objective diagnosis and allow nonexpert endoscopists to achieve a high diagnostic accuracy.

We previously reported that our custom software program can distinguish between images of nonneoplastic and neoplastic lesions in NBI magnifying colonoscopy images.[12] Another study showed the feasibility of computer-based classification of images of colon polyps by using vascularization features.[20] However, these studies were performed by using still images, and they were not performed in real time. Thus, we developed a

computer-aided diagnosis system by using a real-time image recognition system and NBI magnifying colonoscopy. Our custom software uses a bag-of-features representation of local features such as SIFT, followed by SVM classifiers.[12,21,22] A bag-of-features for object recognition was proposed by Csurka et al[23] in 2004 and has since been widely used for general object recognition and image retrieval.[24] The SIFT transforms an image into a large collection of local feature vectors, each of which is invariant to image translation, scaling, and rotation, and partially invariant to illumination changes.[25] SIFT descriptors at sparsely detected key points can be used for recognition; however, densely sampled SIFT descriptors are known to perform better. The densely sampled SIFT descriptors are computed at points on a regular grid and at several scales of the local patch centered at each point. Smaller spacing generates more features while simultaneously increasing the computation and storage cost, ie, consumption of random access memory and the hard drive, but it generally performs better. We used a 5-pixel grid and 5- and 7-pixel scales, as defined by a preliminary study. SVMs are supervised learning models with associated learning algorithms that analyze data and recognize patterns and are used for classification and regression analysis.[26]

Our real-time recognition system analyzed the ROI of the NBI videoendoscopic image in focus without motion blur, and the SVM output values were provided on the screen in real time. In preliminary examinations, when the ROI is large, the range, in addition to the optimum point, is included, and when it is small, precision decreases. Thus, we decided to use an ROI of 200 × 200 pixels. We used an Intel Core i7-4770 CPU 3.4-GHz processor computer (Intel Corp, Santa Clara, Calif), and this system analyzed and displayed the refreshed SVM output value frame-by-frame with high-quality images and a frame rate of 20 frames/s.

The accuracy between diagnosing all lesions by using a real-time image recognition system and by histologic findings was 94.9%, and concordance between diagnosis by a real-time image recognition system and by endoscopists was 97.5%; the κ value between them was excellent. We further evaluated diminutive colorectal lesions. The accuracy between the histologic findings of diminutive colorectal lesions (polyps) and diagnosis by a real-time image recognition system was 93.2%, and the NPV was 93.3%. Colorectal lesions with densely marginal crypt epithelium and sparse blood vessels or attached mucus were considered a false-negative finding. According to our study, agreement of the postpolypectomy surveillance intervals was identical in 38 of 41 patients (92.7%). This finding suggested that our study met the first PIVI recommendation; however, a future prospective, multicenter study on PIVI is needed. The NBI classification of polyps ≤5 mm with a real-time image recognition system may be able to meet both PIVI recommendations.

There are limitations to this study. Magnifying colonoscopy is necessary and requires training. The vast majority of the world does not yet have access to this tool, and this limits the study's generalizability. Thus, further development of our real-time image recognition system, which can analyze nonmagnifying colonoscopy images, is needed, and additional studies aimed at assessing whether community endoscopists may successfully meet both PIVI thresholds are needed.

CONCLUSIONS

Although further investigation is necessary to establish our computer-aided diagnosis system, our findings suggest that this real-time recognition system may predict the histology of colorectal lesions. In addition, the development of our system may make it easier for specialists and community-based gastroenterologists to diagnose colorectal lesions.

ACKNOWLEDGMENTS

The authors thank Shoji Sonoyama for developing the real-time image recognition system. This work was supported by the Japan Society for the Promotion of Science KAKENHI (grants 24591026 and 26280015).

REFERENCES

1. Fearon ER, Vogelstein B. A genetic model for colorectal tumorigenesis. Cell 1990;61:759-67.
2. Fujii T, Rembacken BJ, Dixon MF, et al. Flat adenomas in the United Kingdom: are treatable cancers being missed? Endoscopy 1998;30: 437-43.
3. Rembacken BJ, Fujii T, Cairns A, et al. Flat and depressed colonic neoplasms: a prospective study of 1000 colonoscopies in the UK. Lancet 2000;355:1211-4.
4. Saitoh Y, Waxman I, West AB, et al. Prevalence and distinctive biologic features of flat colorectal adenomas in a North American population. Gastroenterology 2001;120:1657-65.
5. Hamilton SR, Aaltonen LA. World Health Organization classification of tumours: pathology and genetics of tumours of the digestive system. Lyon, France: International Agency for Research on Cancer; 2000. p. 103-42.
6. Rex DK, Kahi C, O'Brien M, et al. The American Society for Gastrointestinal Endoscopy PIVI (Preservation and Incorporation of Valuable Endoscopic Innovations) on real-time endoscopic assessment of the histology of diminutive colorectal polyps. Gastrointest Endosc 2011;73:419-22.
7. East JE, Suzuki N, von Herbay A, et al. Narrow band imaging with magnification for dysplasia detection and pit pattern assessment in ulcerative colitis surveillance: a case with multiple dysplasia associated lesions or masses. Gut 2006;55:1432-5.
8. Tanaka S, Kaltenbach T, Chayama K, et al. High-magnification colonoscopy (with videos). Gastrointest Endosc 2006;64:604-13.
9. Kanao H, Tanaka S, Oka S, et al. Narrow-band imaging magnification predicts the histology and invasion depth of colorectal tumors. Gastrointest Endosc 2009;69:631-6.
10. Tanaka S, Sano Y. Aim to unify the narrow band imaging (NBI) magnifying classification for colorectal tumors: current status in Japan from a

summary of the consensus symposium in the 79th annual meeting of the Japan gastroenterological endoscopy society. Dig Endosc 2011;23: 131-9.
11. Oba S, Tanaka S, Sano Y, et al. Current status of narrow-band imaging magnifying colonoscopy for colorectal neoplasia in Japan. Digestion 2011;83:167-72.
12. Takemura Y, Yoshida S, Tanaka S, et al. Computer-aided system for predicting the histology of colorectal tumors by using narrow-band imaging magnifying colonoscopy (with video). Gastrointest Endosc 2012;75:179-85.
13. Winawer SJ, Zauber AG, Fletcher RH, et al. Guidelines for colonoscopy surveillance after polypectomy: a consensus update by the US Multi-Society Task Force on Colorectal Cancer and the American Cancer Society. Gastroenterology 2006;130:1872-85.
14. Endoscopic Classification Review Group. Update on the Paris classification of superficial neoplastic lesions in the digestive tract. Endoscopy 2005;37:570-8.
15. Rex DK. Management of small and diminutive polyps. Techn Gastrointest Endosc 2013;15:77-81.
16. Tanaka S, Sano Y. Aim to unify the narrow band imaging (NBI) magnifying classification for colorectal tumors: current status in Japan from a summary of the consensus symposium in the 79th Annual Meeting of the Japan Gastroenterological Endoscopy Society. Dig Endosc 2011;23(Suppl 1):131-9.
17. Tanaka S, Oka S, Hirata M, et al. Pit pattern diagnosis for colorectal neoplasia using narrow band imaging magnification. Dig Endosc 2006;18:S52-6.
18. Repici A, Hassan C, Radaelli F, et al. Accuracy of narrow-band imaging in predicting colonoscopy surveillance intervals and histology of distal diminutive polyps: results from a multicenter, prospective trial. Gastrointest Endosc 2013;78:106-14.
19. Ladabaum U, Fioritto A, Mitani A, et al. Real-time optical biopsy of colon polyps with narrow band imaging in community practice does not yet meet key thresholds for clinical decisions. Gastroenterology 2013;144:81-91.
20. Gross S, Trautwein C, Behrens A, et al. Computer-based classification of small colorectal polyps by using narrow-band imaging with optical magnification. Gastrointest Endosc 2011;74:1354-9.
21. Miyaki R, Yoshida S, Tanaka S, et al. Quantitative identification of mucosal gastric cancer under magnifying endoscopy with flexible spectral imaging color enhancement. J Gastroenterol Hepatol 2013;28:841-7.
22. Miyaki R, Yoshida S, Tanaka S, et al. A computer system to be used with laser-based endoscopy for quantitative diagnosis of early gastric cancer. J Clin Gastroenterol 2015;49:108-15.
23. Csurka G, Dance CR, Fan L, et al. Visual categorization with bags of keypoints. Proceedings of the European Conference on Computer Vision (ECCV) 2004;1:1-22.
24. Lazebnik S, Schmid C, Ponce J. Beyond bags of features: spatial pyramid matching for recognizing natural scene categories. Proceedings from the IEEE Conference on Computer Vision and Pattern Recognition (CVPR2006) 2006;2:264-71.
25. Lowe DG. Object recognition from local scale-invariant features. Proceedings from the International Conference on Computer Vision 1999;2:1150.
26. Cortes C, Vapnik V. Support-vector networks. Machine Learning 1995;20:273-97.

T②

Int J Colorectal Dis (2016) 31:571–578
DOI 10.1007/s00384-015-2473-6

ORIGINAL ARTICLE

Long-term outcomes after treatment for T1 colorectal carcinoma

Naoki Asayama[1] · Shiro Oka[2] · Shinji Tanaka[2] · Yuki Ninomiya[1] · Yuzuru Tamaru[1] · Kenjiro Shigita[1] · Nana Hayashi[1] · Hiroyuki Egi[3] · Takao Hinoi[3] · Hideki Ohdan[3] · Koji Arihiro[4] · Kazuaki Chayama[1]

Accepted: 14 December 2015 / Published online: 22 December 2015

Abstract
Purpose Long-term outcomes of patients with T1 colorectal carcinoma (CRC) treated by endoscopic resection (ER) or surgical resection are unclear in relation to the curative criteria in the Japanese Society for Cancer of the Colon and Rectum (JSCCR) guidelines. The aim of this study was to retrospectively compare the long-term outcomes among patients with T1 CRC in relation to the treatment methods.
Methods We examined 322 T1 CRC cases treated between January 1992 and August 2008 at Hiroshima University Hospital. Patients who did not meet the curative criteria in the JSCCR guidelines were defined as "non-endoscopically curable" and classified into three groups: underwent ER alone (group A: 45 patients), underwent additional surgery after ER (group B: 106 patients), and underwent surgical resection alone (group C: 92 patients).
Results Of the 322 T1 CRC patients, 79 were categorized as endoscopically curable and 243 as non-endoscopically curable. Among the endoscopically curable T1 CRC patients, recurrence and 5-year OS rates were 0 and 94.2 %, respectively. In groups A, B, and C, recurrence rates were 4.4, 6.6, and 4.3 %, and OS rates were 85.6, 95.1, and 96.3 %, respectively ($p < 0.05$). Local recurrence or distant/lymph node metastasis was observed in 13 patients (group A: 2; group B: 7; group C: 4). Death due to primary CRC occurred in six patients (group B: 4; group C: 2).
Conclusion Long-term outcomes support the curative criteria according to the JSCCR guidelines. ER for T1 CRC did not worsen clinical outcomes in cases that required additional surgical resection.

Keywords T1 colorectal carcinoma · Treatment · Recurrence · Disease-free survival · Overall survival

Category Colorectal neoplasia.

✉ Shiro Oka
oka4683@hiroshima-u.ac.jp

[1] Department of Gastroenterology and Metabolism, Graduate School of Biomedical Sciences, Hiroshima University, Hiroshima, Japan

[2] Department of Endoscopy, Hiroshima University Hospital, Hiroshima, Japan

[3] Department of Gastroenterological and Transplant Surgery, Applied Life Sciences, Institute of Biomedical and Health Sciences, Hiroshima University, Hiroshima, Japan

[4] Department of Anatomical Pathology, Hiroshima University Hospital, Hiroshima, Japan

Introduction

As a result of recent advances in endoscopic instruments and techniques, the proportion of T1 colorectal carcinoma (CRC) initially treated by endoscopic resection (ER) [1–5] has been increasing. However, lymph node (LN) metastasis occurs in approximately 10 % of T1 CRCs [4–8]. Despite this low likelihood of LN metastasis, surgical resection with regional LN dissection is considered the standard treatment for T1 CRC [9]. It is important to evaluate curability of T1 CRC after ER and determine the indication for additional surgery. According to the Japanese Society for Cancer of the Colon and Rectum (JSCCR) guidelines, the curative criteria of T1 CRC after ER are well/moderately differentiated or papillary carcinoma, no vascular invasion, submucosal invasion depth <1000 μm, and budding grade 1, because of the very low risk of LN metastasis [10, 11]. However, the JSCCR criteria were established based on an analysis of histologic data of T1 CRC from surgically resected specimens [12], and there have been few